J Solid State Electrochem (2016) 20:67–79
DOI 10.1007/s10008-015-2994-5

ORIGINAL PAPER

Electrochemical study of H_3PMo_{12} retention on Vulcan carbon grafted with NH_2 and OH groups

A.K. Cuentas-Gallegos[1] · S. López-Cortina[2] · T. Brousse[4] · D. Pacheco-Catalán[5] · E. Fuentes-Quezada[1,6] · H. Mosqueda[3] · G. Orozco-Gamboa[6]

Received: 24 February 2015 / Revised: 30 June 2015 / Accepted: 24 July 2015 / Published online: 14 August 2015

Abstract In this work, we show a comparative study based on the effects of specific chemical functional groups (–OH, –NH_2), grafted on Vulcan carbon (VC) with the incorporation of a specific polyoxometalate (POM), PMo_{12} ($H_3PMo_{12}O_{40}$), to improve electrochemical performance. We observed a decrease in the specific surface area of the grafted matrices (VC-OH and VC-NH_2) [1], and the same trend was observed for PMo_{12} (POM) incorporation. Our electrochemical studies showed low concentrations of POM in unmodified VCs and higher POM concentrations for grafted matrices (VC-OH and VC-NH_2) after 500 voltammetric cycles, especially for the VC grafted with –OH groups (VC-OH-POM). Mechanisms have been proposed for POM interaction with the grafted groups in carbon, emphasizing the role of aqueous medium and redox activity of POM. Cyclic voltammograms suggested the POM anchoring through –OH groups with a strong interaction as a covalent bond, resulting in a surface coverage of 1.66×10^{-11} mol cm^{-2}. Surface modifications could be extrapolated to other carbons, and the materials could be employed for different potential applications such as photocatalysis, amperometric sensors, fuel cells, and supercapacitors.

Keywords Polyoxometalates · Carbon · Grafting · Hybrid · Nanocomposites

Electronic supplementary material The online version of this article (doi:10.1007/s10008-015-2994-5) contains supplementary material, which is available to authorized users.

✉ A.K. Cuentas-Gallegos
akcg@ier.unam.mx

[1] Instituto de Energías Renovables, Universidad Nacional Autónoma de México, Priv. Xochicalco s/n, Col. Centro, Temixco 62580, Morelos, México

[2] Fac.de Ciencias Químicas, Universidad Autónoma de Nuevo Leon, Av. Universidad s/n, Ciudad Universitaria, CP 66451 San Nicolás de los Garza, Nuevo Leon, México

[3] Fac. de Ing. Mecánica-eléctrica, Universidad Autónoma de Nuevo Leon, Av. Universidad s/n, Ciudad Universitaria, CP 66451 San Nicolás de los Garza, Nuevo Leon, México

[4] Institut des Matériaux Jean Rouxel (IMN), Université de Nantes, CNRS, 2 rue de la Houssinière, BP32229, 44322 Nantes Cedex 3, France

[5] Centro de Investigación Científica de Yucatán A.C., Unidad de Energía Renovable, Calle 43 No. 130 Chuburná de Hidalgo, CP 97200 Mérida, Yucatán, México

[6] Centro de Investigación y Desarrollo Tecnológico en Electroquímica, P. Tecnológico, ZP. 76703 Pedro Escobedo, Querétaro, México

Introduction

Polyoxometalates (POMs) are molecular inorganic metal oxide compounds that exhibit remarkable chemical and physical properties leading to a wide variety of potential applications. In addition, their multielectronic reversible redox reactions, as well as their low cost and toxicity compared to other oxides [2], represent a novel alternative for use in designing nanocomposite materials. Nevertheless, the high solubility of POMs in typical solvents has caused them to be ignored as active compounds for solid-state technology, because they would need to be anchored to a solid framework. POMs with Keggin structure consist of metallic oxide nanoclusters (≈1.5 nm) with formula $[XM_{12}O_{40}]^{3-}$, constructed from a central tetrahedron (XO_4^-, X = non-metal, PO_4^{3-}, SiO_4^{4-}) surrounded by 12 metal-oxygen octahedra linked by shared edges and corners (MO_6, where M = metal, MoO_6, WO_6). These polyanions have been studied in many solid-state applications: heterogeneous catalysis [3–6], amperometric

sensors and fuel cells due to their electrocatalytic properties [7–9], and more recently, in supercapacitors [10–16].

As previously mentioned, the main drawback of POMs in all applications is finding an effective matrix for incorporation where desorption does not take place. In the acidic form, these oxides are known as heteropolyacids, which consist primarily of big polyanions with Keggin structure and also include cations, crystallization water, and other molecules. The 3D arrangement is called the secondary structure; the tertiary structure determines the particle size, surface area, pore size, etc., which establish the final solid-state properties [17]. Heteropolyacids show very small surface areas (1–15 $m^2\ g^{-1}$) and are highly soluble in water. Nevertheless, the surface area can be greatly increased and the pores can be manipulated by metal or cation (Cs^+, NH_4^+, etc.) proton substitutions. The dispersion of heteropolyacids in solid matrices is another method of increasing the surface area and adjusting the porosity, both of which are important in potential solid-state applications. Molecular oxides have been incorporated in different solid matrices, such as zirconia [18], silica [19], alumina [20], TiO_2 [21], and zeolites [3], exhibiting desorption problems due to weak bonding with the matrix. POM particles have also been deposited on electrode surfaces and immobilized into or within conducting polymers to modify their properties [11, 22–26]. Furthermore, they have been incorporated in a diversity of carbon matrices such as activated carbon [15, 16, 27], carbon cloth and fibers [4, 5], gels [6] and aerogels [14], pastes [7, 8], nanofibers [12], multiwalled carbon nanotubes [9–11, 13, 28–33], and graphene [10, 11, 34–37] and electrodeposited onto vitreous carbon substrates [38, 39]. These types of carbon matrices compared to others can strongly immobilize these molecular oxides, showing low solvent desorption due to covalent bonds between the functional groups present on the surfaces of the carbons and oxides [9, 11, 13, 30, 32, 40]. It has been studied that the immobilization, anchoring, or addition of these oxides in the carbon matrices involve a strong and irreversible adsorption [11, 32, 40], which is increased by the microporosity [11, 27] and the hydrophilic nature of the carbon matrix [11], and by the creation of oxygen-based functional groups [9, 11, 13, 30, 32].

Currently, the nature of the specific functional group on the carbon surface that forms covalent bonds with POMs is still unknown. The conventional oxidative treatments that have been used in carbon matrices have not effectively controlled the creation of functional groups; in addition, electric conductivity decreases due to decreased porosity [41]. However, chemical modification of carbon by diazonium salt chemistry (grafting) is a novel procedure that permits selective incorporation of functional groups without destroying porosity. This method consists in the in situ generation of a diazonium cation by diazotization of an aromatic amine and subsequent reduction of the diazonium cation to the corresponding aryl radical, which allows for the modification of the carbon surface with a substituted aryl group, such as in Scheme S1 (supporting information), where *R* is a specific functional group [1, 42–44]. Our previous work confirmed the molecular oxide immobilization through an oxygen-based functional group created during conventional oxidation treatments of the nanocarbons' surface [9, 12, 13, 31–33]. Therefore, the intrinsic oxidative nature of POMs and their acidity could be responsible for the interaction with the functional group in question. In this work, we show a comparative study between the bare Vulcan carbon matrix and its modification with grafted functional groups on POM retention. We have selected the –OH group as a model group to graft on Vulcan carbon, because it represents the least oxidized functional group of all oxygen-based groups. In addition, interactions of the molecular oxides have previously been reported with amine groups over silica [45–47], amine groups in polyaniline [24, 25], polypyrrole [48], and polyethylenimine [49]. Therefore, we also grafted an amine group onto the carbon matrix. Grafting functional groups on the surface of carbons enables us to monitor the surface chemistry, which is a useful information for POM attachment.

Experimental section

Grafting of –NH_2 and –OH groups

We used Vulcan carbon (VC; Black VXC-72) from Química Rana, *p*-phenylenediamine (precursor of NH_2 groups), 4-aminophenol (precursor of OH groups), and sodium nitrite (97 %+) from Sigma-Aldrich, as well as analytical grade solvents. The procedure for grafting –NH_2 and –OH groups on VC was performed similar to the work of Lyskawa et al. [50] and can be summarized as follows: 500 mg of VC was dispersed in 50 ml of deionized water using an ultrasonic bath for 10 min; then, 4 mmol of the specific functional group aminophenyl precursor (φ-NH_2 or φ-OH) and two drops of HCl (37.1 % from Fermont) were added. The solution was stirred for 1 h to adsorb the precursor or corresponding amine on the carbon. Subsequently, 4 mmol of $NaNO_2$ dissolved in 50 ml of deionized water were added to the solution to reduce the aminophenyl precursor, and the reaction was stirred for 16 h under N_2 bubbling. The resulting suspension was filtered under vacuum and rinsed with H_2O, acetonitrile, dimethylformamide, and methanol solvents to remove excess unreacted reagents. The solids were dried at 353 K for 1 h.

POM incorporation

The synthesis to incorporate phosphomolybdic acid ($H_3PMo_{12}O_{40}\ nH_2O$ from Fermont (PMo_{12})) into the different carbon matrices was performed as follows: each carbon matrix (VC, VC-NH_2, and VC-OH) was sonicated in 50 ml of 1.0 mM PMo_{12}/H_2O or EtOH solution for 1 h in an ultrasonic

bath; it was then vacuum filtered and washed using the respective solvent (H_2O or EtOH). The different materials obtained are described below (see Table 1).

ATR and FTIR analyses

We performed attenuated total reflectance (ATR) spectra for all carbon matrix materials (VC, VC-NH_2, and VC-OH) and Fourier transform infrared (FTIR) spectra for the best POM-incorporated materials (VC-NH_2-POM and VC-OH-POM in aqueous medium) in KBr pellets to confirm the presence of grafted functional groups and the incorporation of POM. We used a Thermo Scientific Nicolet 8700 spectrometer with a frequency interval between 4000 and 650 cm^{-1}.

BET surface area

We performed nitrogen isotherm measurements at 77 K for all materials with a Quantachrome NOVA instrument. Prior to the measurements, we purged the samples under vacuum at 393 K for 16 h to clean the surface and prevent PMo_{12} degradation at higher temperatures. To calculate the specific surface area (S_{BET}), *we analyzed the nitrogen isotherms by the Brunauer-Emmett-Teller (BET) theory between 0.02 and 0.3* P/P_o.

Electrochemical characterization

We performed the electrochemical studies at room temperature (298 K) in a conventional three-electrode system using cyclic voltammetry in a Biologic VSP potentiostat controlled by EC-Lab® software. The three electrodes in our system were a Hg/Hg_2SO_4 reference electrode (SSE), a platinum coil counter electrode, and our different materials as the working electrode. Each working electrode was prepared as follows: in ethanol, we mixed 60 wt.% of our sample material, 30 wt.% Super P conductive carbon (brand TIMCAL Graphite and Carbon), and 10 wt.% Teflon (Sigma-Aldrich) as a binder and heated it until it was fully evaporated to obtain a black dough. The dough was cold rolled to prepare a film, which was then dried at room temperature for 24 h to eliminate residual ethanol. The films were cut into 1-cm^2 squares and pressed in a stainless steel wire cloth current collector (Aisi 316 L 250 wire, 160 μ). The mass loading was typically between 3 and 5 mg cm^{-2}. The 0.5 M H_2SO_4 electrolyte was first purged with highly purified N_2 for at least 20 min, and the voltammograms are shown in terms of normal hydrogen electrode (NHE) by performing the pertinent conversion (V vs SSE + 0.65 V = V vs NHE).

Results

Grafting –NH_2 and –OH groups

We obtained ATR spectra for all the carbon matrices in order to confirm the incorporation of the grafted functional groups (Fig. 1). The VC matrix spectrum showed a band at ~3332 cm^{-1} related to OH stretching, indicating the presence of an –OH functional group and/or water adsorbed on the surface of the sample [51, 52]. In addition, we observed bands at 2916 and 2850 cm^{-1} corresponding to the C–H stretching of the methyl and methylene [52, 53], bands at 1643 and 1534 cm^{-1} assigned to C=C and C–C stretching conjugated benzene ring bonds [52, 54], and bands at 908 and ~753 cm^{-1} assigned to –C=CH_2 (terminal bonds) and C–H bending (off plane). For the modified carbon with φ-NH_2 (VC-NH_2), in addition to the same peaks seen in the VC spectrum, we observed a sharper band at 3300 cm^{-1} corresponding to N–H stretching, a band at 709 cm^{-1} assigned to N–H wag, a band at 1240 cm^{-1} assigned to C–N stretch in aromatic amines out of the plane (Ar-NH_2), and a band at 1075 cm^{-1} corresponding to C–N stretching of amine group or of secondary amines [53–55]. We must note that the peak at 3300 cm^{-1} could indicate exclusively –OH functional groups, and if this is the case, the presence of secondary amines could not be ruled out. The X-ray photoelectron spectroscopy surface analysis (Fig. S1, supporting information) for VC-NH_2 clearly demonstrates the presence of –NH_2-grafted functional groups indicated from a N1s peak centered at 399.6 eV, unlike the pristine carbon sample, which does not exhibit a peak at this binding energy.

Finally, for the carbon matrix grafted with φ–OH groups (VC-OH), we observed a wider signal at 3200 cm^{-1} compared to the signal in the unmodified VC spectrum; this is assigned to –OH stretching with H bonded. We also observed a band at 1153 cm^{-1} assigned to C–O stretching in aromatics (Ar-OH) [54, 56] and a shoulder at approximately 1000 cm^{-1} assigned to C–O bond, in good agreement with previous work on grafted –OH groups [57]. The extra ATR peaks observed in the VC-NH_2 and VC-OH spectra confirm that the bare carbon matrix (VC) was grafted with –NH_2 (VC-NH_2) and –OH (VC-OH) groups.

Table 1 Prepared materials

Carbon matrix	Vulcan carbon (VC)	VC-NH_2	VC-OH
POM incorporation	VC + POM/H_2O	VC-NH_2 + POM/H_2O	VC-OH + POM/H_2O
	VC + POM/EtOH	VC-NH_2 + POM/EtOH	VC-OH + POM/EtOH

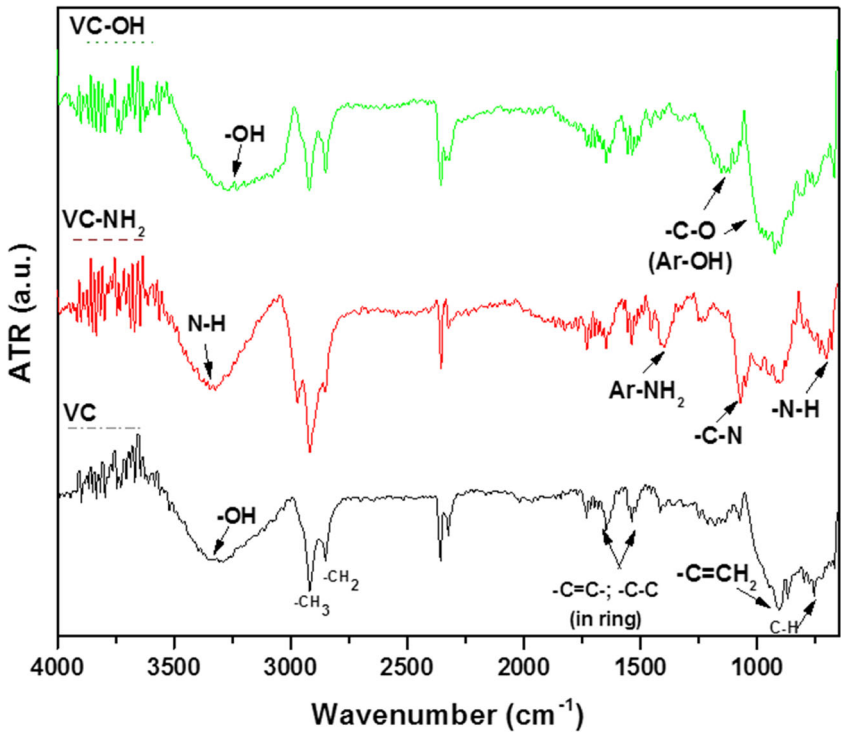

Fig. 1 ATR spectra of the grafted carbons with $–NH_2$ and –OH ($VC-NH_2$ and VC-OH, respectively) and the bare carbon matrix (*VC*) as a reference

We calculated BET surface areas using N_2 isotherms between 0.02 and 0.3 P/P_o (Fig. S2, supporting information) for all of the prepared materials, resulting in 221 $m^2\ g^{-1}$ for the unmodified VC matrix. The isotherm starting points revealed the microporous nature of the materials; in Table 2, we list the calculated BET surface areas for all of the samples. We observed a decrease in the BET surface areas after grafting φ-NH_2 and φ-OH groups on VC (161 and 181 $m^2\ g^{-1}$, respectively). This finding suggests that the grafted functional groups block in some degree the micropores observed in the unmodified VC matrix, as we can observe by the volume decrease in the BET isotherm at the starting point, and the unchanged slope of the adsorption isotherm (mesoporosity), in good agreement with previous work by Pognon et al. [1] on anthraquinone grafting. When looking at the surface area (Table 2) occupied by the functional groups compared with the unmodified VC matrix, the $VC-NH_2$ matrix shows the greatest loss of surface area (≈60 $m^2\ g^{-1}$), followed by VC-OH matrix surface area loss (≈40 $m^2\ g^{-1}$); the losses are most likely due to the size of the functional group.

POM incorporation

We performed FTIR analyses and N_2 isotherms in order to confirm POM incorporation to the different VC matrices. The vibrational modes of FTIR spectrum of unbind POM are presented at 1064 cm^{-1} for P–O, at 962 cm^{-1} for Mo = O (terminal oxygen), at 868 cm^{-1} for vertex or corner Mo–O, and at 783 cm^{-1} for edge Mo–O [32], which are in good agreement with the spectrum inset shown in Fig. 2. FTIR spectra confirmed the presence of POM in the pristine carbon matrix (VC, Fig. S3a) and grafted matrices (VC-OH, Fig S3b; VC-NH2, Fig S3c). In Fig. 2, we show the spectra for the samples obtained with the grafted carbon matrices in aqueous medium, which are representative of all obtained spectra (Fig. S3). The information that we can extract is that no significant change was observed in the pristine VC (Fig. S3a) nor in the $VC-NH_2$ matrix when POM was incorporated (Fig. S3c), while in VC-OH matrix, important changes were detected. The wider signal at 3200 cm^{-1} detected in VC-OH matrix (Fig. 1) disappeared, as well as the vibrational bonds related with OH groups (1153 cm^{-1} and around 1000 cm^{-1} assigned to C–O bond in aromatics, Fig. S3b).

POM incorporation in the micropores of materials exposed to different POM solutions (Fig. S2, decrease of the isotherm starting point) contributes to smaller observed values of S_{BET}

Table 2 BET surface area values obtained from N_2 adsorption isotherms between 0.02 and 0.3 P/P_o for all VC-based materials

Sample	$S_{BET}/m^2\ g^{-1}$		
	Carbon matrices	Aqueous media	Ethanol media
VC	221.72	–	–
$VC-NH_2$	161.94	–	–
VC-OH	181.48	–	–
VC + POM		184.11	117.21
$VC-NH_2$ + POM		88.73	102.01
VC-OH + POM		109.36	124.19

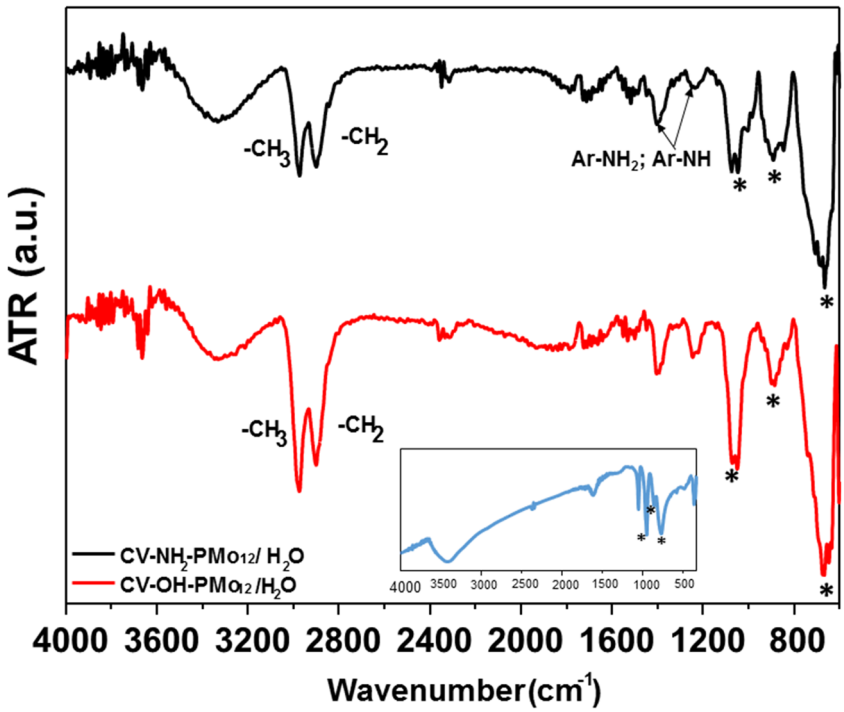

Fig. 2 FTIR spectra of as-prepared materials with POM incorporation using aqueous media (CV-NH_2–POM/H_2O and CV-OH–POM/H_2O) in KBr pellets. Vibrational modes of POM are marked with an *asterisk*

compared with the respective matrices without POMs (Fig. S2; Table 2). The decreases in S_{BET} ≈72–73 $m^2\ g^{-1}$ (Fig. S2a) in an aqueous medium is likely due to POM occupation and were greater than the loss seen for the ethanol, where the decrease in the S_{BET} was ≈57–60 $m^2\ g^{-1}$ (Fig. S2b). The large decrease observed from samples in the aqueous media is most likely due to the interactions of –NH_2 and –OH groups with water (OH^- and H^+) facilitating POM incorporation. Surprisingly, a major decrease in surface area (≈105 $m^2\ g^{-1}$) was observed for the bare VC matrix when exposed to POM in ethanol. This observation will be explained herein.

Electrochemical characterization

In Fig. 3, we show the cyclic voltammograms of the unmodified VC, VC-NH_2, and VC-OH matrices in 0.5 M H_2SO_4 at a scan rate of 100 mV s^{-1}. For the VC matrix, we observed a rectangular shape voltammogram that is characteristic of a carbon electrode with an electrochemical double-layer formation. For the VC-OH matrix, we observed two redox pairs of broad peaks at 0.33/0.44 V (a/a′) and smaller at 0.60/0.68 V (b/b′). They have been previously assigned to a faradaic contribution from oxygen-based functional groups [58], and the following redox reaction has been proposed [59, 60]:

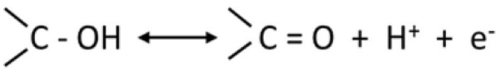

In the VC-NH_2 matrix, we observed a larger redox pair at approximately −0.01/0.22 V (c/c′) and a smaller one at 0.56/0.72 V (b/b′) related to amine protonation-deprotonation. Previous research on electro-active nitrogen-containing functional groups electrochemically characterized in similar conditions detected a broad redox pair contribution (reduction approximately −0.341 to −0.041 V and oxidation −0.041 to 0.359 V) in carbon nanotubes doped with N [61], a redox couple (0.149 V/0.19 V) related with the electroactivity of grafted diphenylamine (DPA) on to a glassy carbon electrode [62], and a specific redox couple (−0.041 V/0.189 V) related with *p*-aminodiphenylamine (ADPA) [63]. If we consider the possibility of secondary amines present in the VC-NH_2 matrix, as suggested by the ATR spectrum, the redox couple c/c′

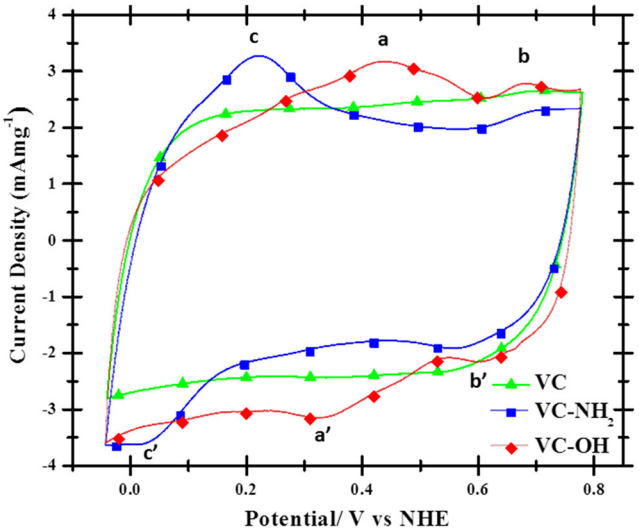

Fig. 3 Cyclic voltammograms of the VC (*filled triangles*), VC-NH_2 (*filled squares*), and VC-OH (*filled diamonds*) electrodes in a 0.5 M H_2SO_4 solution at 100 mV s^{-1}

could correlate to the presence of aniline dimers (DPA and ADPA) in addition to the aniline grafted to the VC matrix, as shown in Scheme 1.

The presence of aniline dimers in the grafted carbon VC-NH_2 is thought to come from the *p*-phenylenediamine precursor not being homogeneously adsorbed on the carbon surface, giving way to multilayer formation by coupling between the attached groups and the radicals in solution, and in some degree clogging the pores. Belanger et al. [64] claimed that the amino group is a good nucleophile that can react with the $–N_2^+$ group when nitrate is added during the grafting procedure, resulting in aniline dimers. The formation of these dimers may explain the major decrease in surface area observed for VC-NH_2. Additional work is needed to better understand the grafting procedure phenomena resulting in the improved electrochemical performance of the carbon electrode. In general, the extra redox peaks observed for both grafted matrices (VC-OH and VC-NH_2) reveal the modification of the bare VC matrix during the grafting procedure [65].

In Fig. 4, we show the cyclic voltammograms from 500 cycles of the POM-incorporated materials at the same potential and scan rate conditions as in Fig. 3. We will first discuss the different contributions observed in the first few cycles for all VC matrices exposed to POM aqueous or EtOH solutions, followed by the evolution of the voltammograms over 500 cycles. In these voltammograms, we observed three redox peaks marked as I/I′, II/II′, and III/III, compared with the corresponding unincorporated matrix. The redox pairs appeared around ≈0.43/0.58 V (I/I′), ≈0.3/0.45 V (II/II′), and ≈0.05/0.18 V(III/III′) and correspond to the characteristic electrochemical redox pairs of this particular POM ($PMo_{12}O_{40}$), as shown in Scheme 2 [15, 16, 31], confirming the presence of POMs.

For the bare VC matrix treated with the POM aqueous solution (VC + POM/aqueous, Fig. 4a), we observed retention of the double-layer behavior of the carbon matrix without any important modifications. This finding indicates that POM treatment did not result in the matrix oxidation commonly observed in extended reaction times [15, 16, 40] and did not block accessible pores. However, when the same matrix was treated with a POM/EtOH solution (VC + POM/EtOH, Fig. 4b), a decrease of the double layer was observed. This result suggests that oxidation of VC by POMs or modification of VC, resulting in lost BET surface area (Table 2), is facilitated in ethanol. In the grafted electrodes (VC-NH_2 and VC-OH) treated with a POM aqueous solution (VC-NH_2 + POM/aqueous and VC-OH + POM/aqueous, Fig. 4c, e), we observed the characteristic POM redox peaks, which seemed more irreversible for VC-NH_2 + POM/H_2O electrode (redox pairs with increased separation, III/III′). On the other hand, VC-OH + POM/H_2O electrode shows additional peaks (b/b′) related with the grafted OH group as described in Fig. 3 and an additional peak around 0.2/0.25 V that will be later described. In addition, the current density of the voltammetric profiles compared to the corresponding grafted carbon matrix and unmodified carbon matrix (VC) increases. The presence of additional current suggests that the grafted functional groups facilitate the incorporation of POM in an aqueous medium without a detrimental effect on the electrochemical behavior of the carbon matrix. However, when we performed the POM treatment of the grafted matrices in ethanol, the current density increase for the VC-NH_2 + POM/EtOH electrode (Fig. 4d) was small and no increase was observed for the VC-OH + POM/EtOH electrode (Fig. 4f). We must note that the POMs are being incorporated, but the effect on the current density

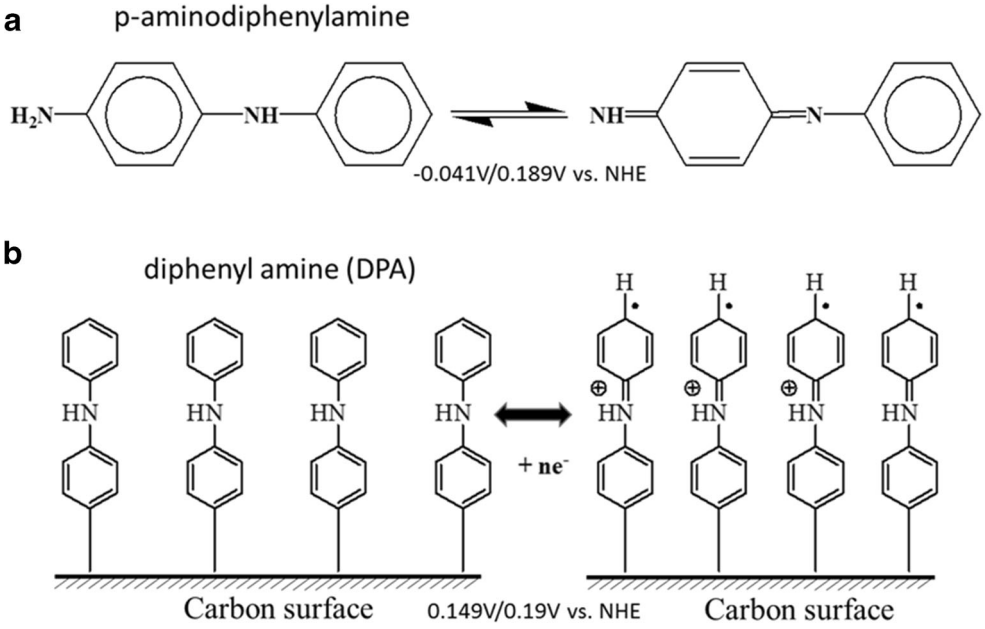

Scheme 1 Schematic representation of aniline dimer redox pairs, possibly involved in the carbon matrix modified with –NH_2 groups (VC-NH_2). Adapted from the work of Santos et al. [62] and Sharma et al. [63]

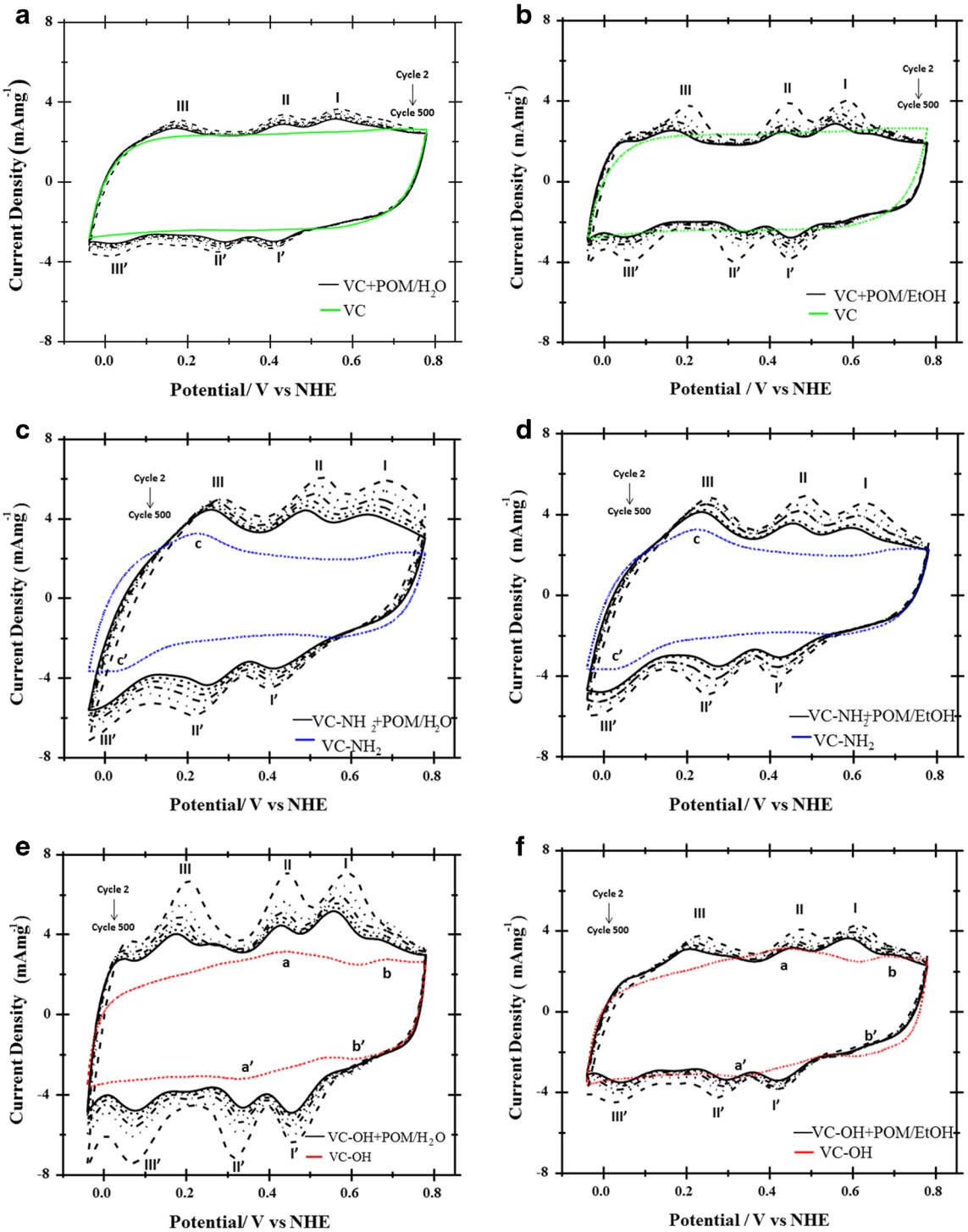

Fig. 4 Cyclic voltammograms of all POM-treated electrodes characterized in a 0.5 M H_2SO_4 solution at 100 mV s^{-1}, were cycles 2, 100, 200, 300, 400, and 500 are shown, as the voltammogram of the corresponding carbon matrices (*colored lines*). Carbon matrices treated with POM aqueous solutions are shown in **a** bare VC matrix (VC + POM/H_2O), **c** grafted matrix with NH_2 (VC-NH_2 + POM/H_2O), and **e** grafted matrix with –OH (VC-OH + POM/H_2O), and the same matrices treated with POM alcohol solutions are shown in **b** bare VC matrix (VC + POM/EtOH), **d** grafted matrix with NH_2 (VC-NH_2 + POM/EtOH), and **f** grafted matrix with –OH (VC-OH + POM/EtOH)

again suggests that POM incorporation in ethanol does not yield optimal materials.

From the cyclic voltammograms shown in Fig. 4, we observed that the POM redox peaks decreased upon cycling and stabilized after 500 cycles. This finding indicates that partial POM desorption takes place resulting from weak bonds with the carbon matrix (physisorption), such as electrostatic interactions. Nevertheless, the most important parameter to

$$PMo_{12}{}^{VI}O_{40}{}^{3-} + 2e^- + 2H^+ \rightleftharpoons H_2PMo_2{}^{V}Mo_{10}{}^{VI}O_{40}{}^{3-} \quad I/I'$$

$$H_2PMo_2{}^{V}Mo_{10}{}^{VI}O_{40}{}^{3-} + 2e^- + 2H^+ \rightleftharpoons H_4PMo_4{}^{V}Mo_8{}^{VI}O_{40}{}^{3-} \quad II/II'$$

$$H_4PMo_4{}^{V}Mo_8{}^{VI}O_{40}{}^{3-} + 2e^- + 2H^+ \rightleftharpoons H_6PMo_6{}^{V}Mo_6{}^{VI}O_{40}{}^{3-} \quad III/III'$$

Scheme 2 Schematic representation of the three characteristic POM redox pairs

determine is which matrix retains the highest POM concentration. To estimate the percentage of desorbed and retained POM during cycling across all matrices, we calculated the difference between the total charge of the 2nd and 500th cycles. In Fig. S4 (supporting information), we show the results of these calculations for the aqueous and ethanol media. Higher percent of POM loss was observed for the aqueous medium versus ethanol for the grafted matrices, and the opposite was true for the unmodified matrix (VC). Nevertheless, we observed that all of the carbon matrices treated with the aqueous POM solution showed higher POM retention concentrations after 500 cycles in comparison with the ethanol-treated samples. The grafted matrices also retained higher POM concentrations compared to the unmodified matrix. The matrix grafted with –OH groups (VC-OH) exhibited the highest POM retention (VC-OH-POM). These results confirm that grafting carbon with functional groups, such as $–NH_2$ or –OH, promotes higher POM retention.

In Fig. 5a, we show the cyclic voltammograms at different scan rates of the best electrode (higher POM retention), VC-OH-POM/H_2O. The characteristic POM redox pairs (I/I′, II/II′, and III/III′) were present at lower scan rates (10 mV s^{-1}) and remained up to 200 mV s^{-1}, indicating the fast response of the redox behavior of POM incorporated in this carbon matrix. Nevertheless, we must note that at high scan rates, the reduction and oxidation peaks tend to separate, indicating less reversibility compared to lower scan rates. In addition, we observed an extra peak at all scan rates (previously detected in Fig. 4e in cycle 500), which we marked with an asterisk. This extra peak was previously observed by Fernandes et al. [36] and was related with the formation of β-isomers of POM that are oxidized at more positive potentials than the corresponding α-isomers. Furthermore, Fig. 5b shows the current density of the reduction and oxidation process of the I/I′ redox pair versus the scan rate. A proportional increase of the current densities (oxidation, reduction) with the scan rate confirm that POMs are not being dissolved (desorbed) during cycling but are rather anchored to this grafted matrix through a stronger interaction as in a covalent bonding, improving the presence of POMs on the surface of the electrode.

To calculate the POM coverage of the grafted carbon matrix, we calculated the slope of each line (Fig. 5b) using the geometrical area (1 cm^2) of the electrode according to the work of Martel et al. [66]. Then, the mass loading of functionalized carbon per geometric surface area of this electrode (≈3.4 mg cm^{-2}) and the BET-specific surface area for the VC-OH-POM sample (109 m^2 g^{-1}) was considered, corresponding to 1.66×10^{-11} mol cm^{-2} of carbon. Although this

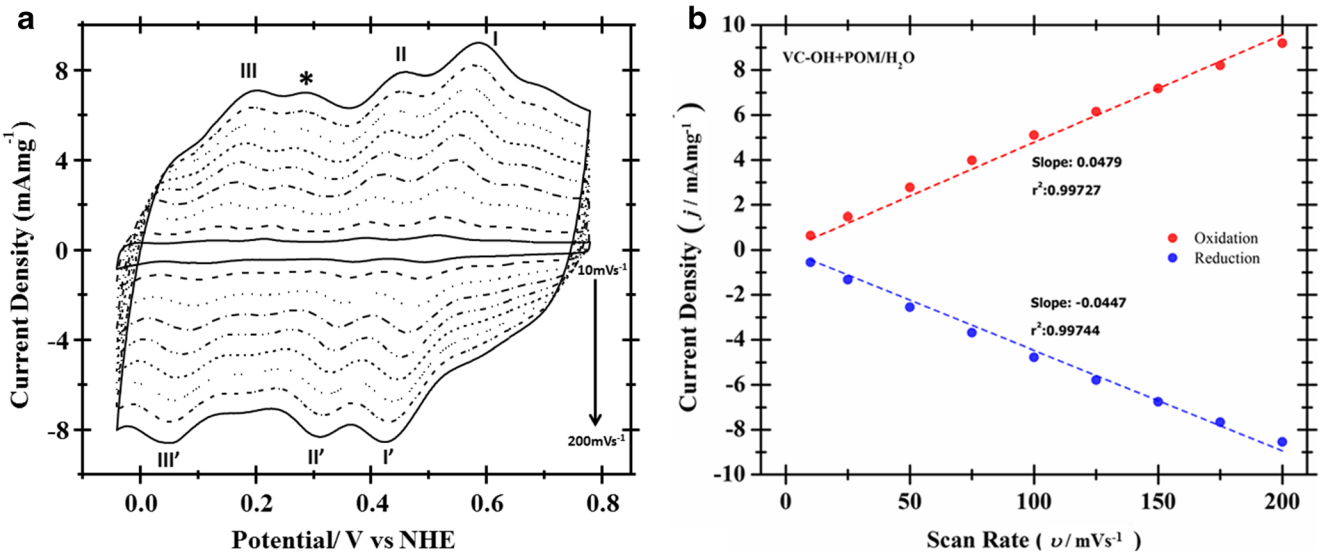

Fig. 5 **a** Cyclic voltammograms of the VC-OH−POM/H_2O electrode in a 0.5-M H_2SO_4 solution at different scan rates (10, 25, 50, 75, 100, 150, 175, and 200 mV s^{-1}). **b** Middle oxidation and reduction peak (I/I″) current plotted as a function of the scan rate

value may appear low compared to literature values of functionalized carbon using diazonium chemistry and spontaneous chemical grafting (10^{-9} to 10^{-10} mol cm^{-2}) [42–44], one must account for the POM surface area and volume, which are much larger than conventional grafted molecules. The projected surface area of a POM anion is close to 1.76 nm^2, almost 28 times higher than conventional phenyl-based grafted radicals. This outcome is evidence of the optimized surface coverage of carbon by POMs, which are attracted by the φ-OH radical grafted at the carbon surface. Therefore, coverage of 1.66×10^{-11} mol cm^{-2} of the carbon surface suggests that an optimized amount of POM has been grafted using our chemical process.

Discussion

Until now, we observed better POM incorporation in aqueous media than in alcohol media. In this regard, we can mention the specific characteristic of heteropoly acids (HPA) such as phosphomolybdic acid, which are greatly soluble in polar solvents as well as being fully dissociated in aqueous solution which gives the strong acidity [2]. In addition, the effect of water amount on the acidity of POM in water-organic solutions has been previously reported, in which the acidity decreases upon addition of water, then goes through a minimum and then increases with further increase of water concentration [67]. This behavior of phosphomolybdic acid could be related to the mechanism of its incorporation into different carbon matrices.

Specifically for the VC-OH matrix (Scheme 3), we could propose the interaction of phenolic OH group with water molecules by the transfer of proton to water showing an equilibrium between these species [68]. In addition, because of the presence of fully dissociated POM in water, the matrix could present protonated –OH groups, allowing electrostatic interactions between this positively charged species and anionic phosphomolybdate.

In this regard, we consider the dissociation of phosphomolybdic acid as a relevant factor, emphasizing that in aqueous media, the acidic protons could be more available for –OH protonation than the acidic protons in ethanol media [67]. In addition, the softness of heteropolyanions (anionic phosphomolybdate), plays an important role in stabilizing organic intermediates such as the protonated forms of VC-OH matrix [2].

The oxidative effect of POM must be included in the mechanism of POM incorporation. The oxidation of phenolic groups could generate phenoxyl radical, and the presence of radical coupling should not be ruled out [68]. The intrinsic oxidative nature of POM could also be responsible for some covalent interaction with the functional group present in the matrix (OH in this case). This proposed reaction mechanism involving a covalent bond is currently under study by theoretical calculations.

On the other hand, for VC-NH_2 matrix, aqueous media also facilitates POM incorporation compared to ethanol media. As

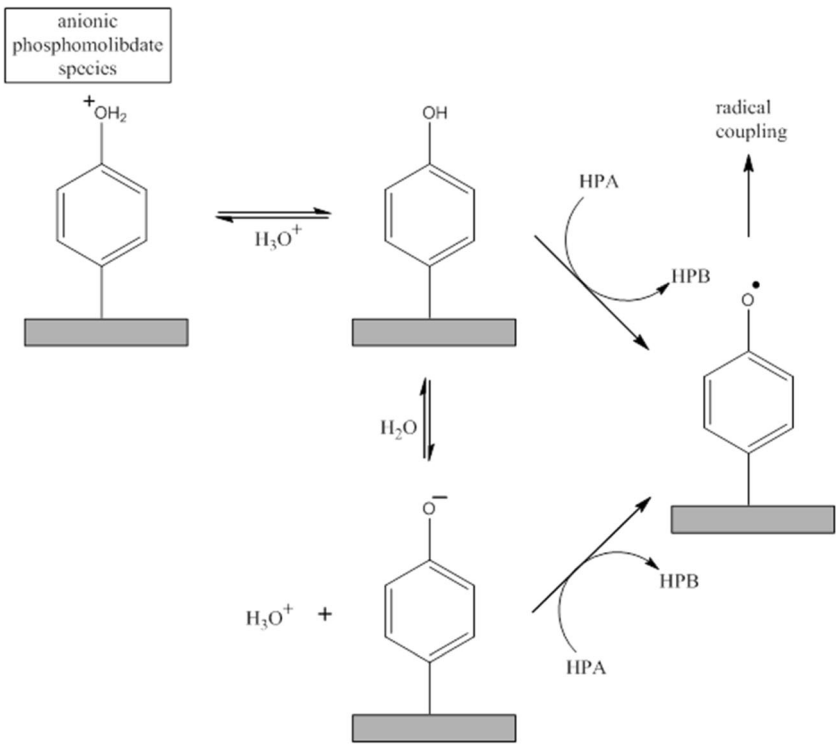

Scheme 3 General proposed mechanism of POM incorporation in VC-OH matrix in aqueous media. (*HPA* heteropoly acid, *HPB* reduced heteropoly acid)

we mentioned above, full dissociation of phosphomolybdic acid in aqueous media should be considered as a crucial factor (Scheme 4). In this regard, we could propose a mechanism in which the VC-NH_2 (primary or secondary amine group) is present in the protonated form stabilized by electrostatic interaction with anionic phosphomolybdate. The oxidation of VC-NH_2 matrix could be carried out as well as the expected reduction of POM, resulting in a stronger interaction.

It is important to note that the proposed electrostatic interaction, between the anionic phosphomolybdate and the protonated grafted groups, is considered a weak interaction and could be related with the higher POM desorption (Fig. S4a). Nevertheless, in aqueous medium, a higher POM retention was observed as previously mentioned and must be related with the oxidative properties of POM resulting in a stronger interaction with these grafted matrices.

We performed FTIR analyses of VC-NH_2-POM and VC-OH-POM samples prepared in aqueous medium using KBr pellets (Fig. 6). These samples were washed several times with deionize water to remove weakly bonded POM (physisorption) and try to identify any shifts of the POM and grafted groups vibrational modes that could be related to any covalent bond. In both samples, we can observe these characteristic POM vibrational modes, where the P–O bond is observed around 1066 cm^{-1} as a wide and intense band due to the overlapping with the characteristic C–N stretching

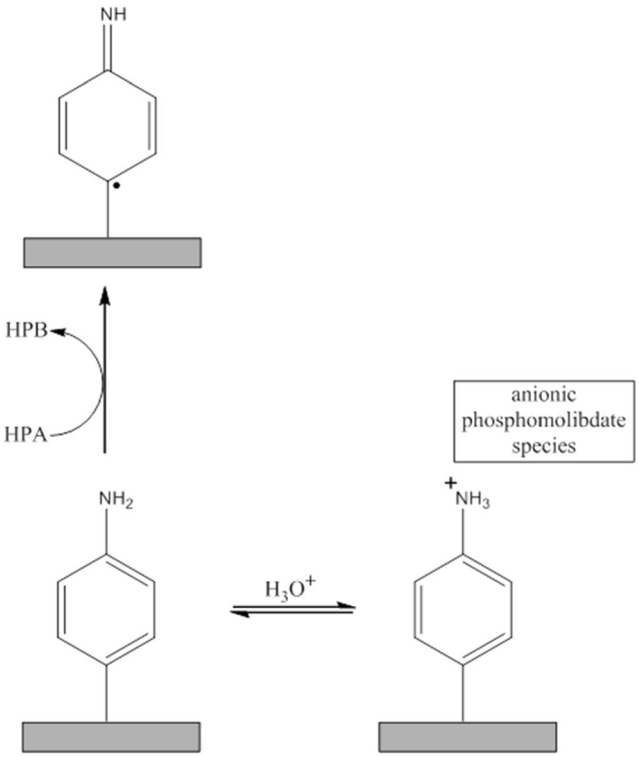

Scheme 4 General proposed mechanism of POM incorporation in VC-NH_2 matrix in aqueous media. (*HPA* heteropoly acid, *HPB* reduced heteropoly acid)

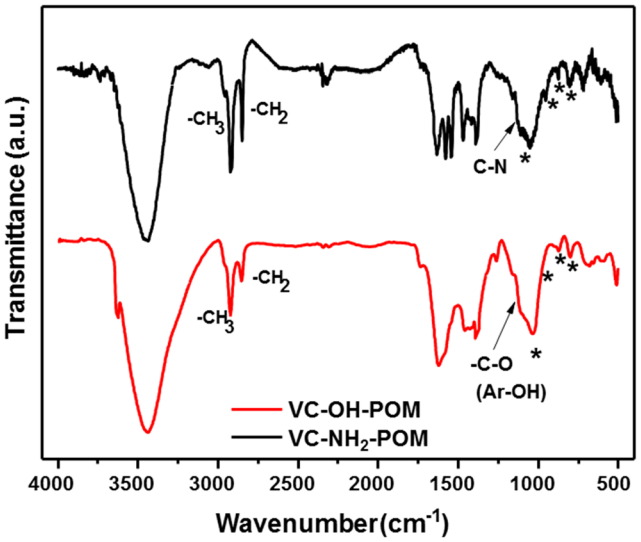

Fig. 6 FTIR spectra of washed materials with deionize water (CV-NH_2–POM/H_2O and CV-OH–POM/H_2O) in KBr pellets. Vibrational modes of POM are marked with an *asterisk*

(1075 cm^{-1}) of the grafted amine group for VC-NH_2-POM spectrum, and the presence of C–O stretching (Ar-O-R, 1153 cm^{-1}) [54–57] for VC-OH-POM spectrum. For sample VC-NH_2–POM, the Mo=O terminal bond is observed at 956 cm^{-1}, while the vibrational modes corresponding to Mo–O corner (vertex) and edge bonds are observed at 868 and 801 cm^{-1}. In the case of VC-OH–POM sample, the Mo=O terminal bond is overlapped with the wide band including the vibrational modes of P–O and C–O bonds, and the vibrational modes related with Mo–O corner and edge bonds are observed at 869 and 805 cm^{-1}. The major shift of POM vibrational modes in these grafted matrices was observed for Mo–O edge bond (from 783 to around 800 cm^{-1}), and also a smaller shift of Mo=O band was observed in the VC-NH_2–POM spectrum. These changes suggest that Mo–O edge bond and probably Mo=O bond in POM are the ones involved in the covalent bonding with the grafted matrices, as observed previously in our earliest work with other carbon matrices [53], and anchoring in conducting polymers [69, 70]. On the other hand, the shifts of the bands related with the grafted groups are difficult to extract due to overlapping. Therefore, ongoing theoretical work will try to get more insight on how POM clusters are oriented on the substrate surface as well as the nature of the charge transfer between the POM molecule and the carbon support.

Conclusions

We show a comparative study based on modified VC carbon matrices by grafting diazonium derivatives to incorporate –NH_2 and –OH groups, resulting in higher POM retention. We observed that the grafting procedure partially blocked the

micropores of the bare VC matrix, and the modifications were confirmed by ATR and cyclic voltammetry. We must note that our $–NH_2$ grafting procedure could also result in the incorporation of aniline dimers, as suggested from the cyclic voltammetry results and previous work [64]. In POM-treated matrices, we detected higher surface area losses for grafted matrices versus the unmodified VC due to higher POM concentrations. In addition to improvements in POM retention in the grafted matrices over 500 voltammetric cycles, we observed that an aqueous medium was better than ethanol at facilitating POM retention, and the POM desorption phenomena pertains to weakly bonded POMs through electrostatic interactions (physisorption). These weak interactions have been included in the proposed interaction mechanisms using aqueous medium, where protonation of grafted groups are considered. Our results show that the matrix retaining the highest concentration of POMs was the VC-OH matrix in aqueous medium (VC-OH−POM-H_2O), where POM redox couples are present with good kinetic behavior. We suggest that the anchoring of POMs in the VC-OH matrix is being facilitated by the electrostatic interaction in aqueous medium, promoting a higher concentration of covalent-bonded POM where the oxidative nature of POM must be involved. A POM coverage of 1.66×10^{-11} mol cm^{-2} has been calculated for our best material (VC-OH−POM-H_2O). Our POM-retaining carbon matrix methodology could be extrapolated to other carbon materials for various potential applications, such as photocatalysis, amperometric sensors, fuel cells, and supercapacitors.

Acknowledgments We acknowledge the technical work of Patricia Altuzar-Coello and Rogelio Morán Elvira from Instituto de Energías Renovables-Universidad Nacional Autónoma de México, Jorge Dominguez Maldonado from Centro de Investigación Científica de Yucatan, and Julio Mata Salazar and Dr. Alberto Herrera from CINVESTAV-Queretaro. Additionally, we are grateful for the financial support granted from Consejo Nacional de Ciencia y Tecnología Basic Science Project 154259, Project IN105410 and IN112414 from Programa de Apoyo a Proyectos de Investigación e Innovación Tecnológica. We would also like to thank the University of Nantes for providing invited professorship to AKCG.

References

1. Pognon G, Brousse T, Bélanger D (2011) Effect of molecular grafting on the pore size distribution and the double layer capacitance of activated carbon for electrochemical double layer capacitors. Carbon 49:13401348
2. Kozhevnikov IV (1998) Catalysis by heteropoly acids and multicomponent polyoxometalates in liquid-phase reactions. Chem Rev 98:171–198
3. Pourbeyram S, Moosavifar M, Hasanzadeh V (2014) Electrochemical characterization of encapsulated polyoxometalates (POMs) into the zeolite. J Electroanal Chem 74:19–24
4. Xu L, Boring E, Hill CL (2000) Polyoxometalate-modified fabrics: new catalytic materials for low-temperature aerobic oxidation. J Catal 195:394–405
5. Lu TT, Xu XX, Li HL, Li ZY, Zhang X, Jz O, Mei ML (2015) The loading of coordination complex modified polyoxometalate nanovelts on activated carbon fiber: a feasible strategy to obtain visible light active and highly efficient polyoxometalate based photocatalyst. Dalton Trans 44:2267–2275
6. Mukai SR, Sugiyama T, Tamon H (2003) Immobilization of heteropoly acids in the network structure of carbon gels. Appl Catal A 256:99–105
7. Wang X, Wang E, Lan Y, Hu C (2002) Renewable PMo12-based inorganic–organic hybrid material bulk-modified carbon paste electrode: preparation, electrochemistry and electrocatalysis. Electroanal 14:1116–1121
8. Liu H, He P, Li Z, Sun C, Shi L, Liu Y, Zhu G, Li J (2005) An ionic liquid-type carbon paste electrode and its polyoxometalate-modified properties. Electrochem Commun 7:1357–1363
9. Cuentas-Gallegos AK, Miranda-Hernández M, Vargas-Ocampo A (2009) Dispersion effect of Cs-PW particles on multiwalled carbon nanotubes and their electrocatalytic activity on the reduction of bromate. Electrochim Acta 54:4378–4383
10. Ji Y, Huang L, Hu J, Streb C, Song YF (2015) Polyoxometalate-functionalized nanocarbon materials for energy conversion, energy storage and sensor systems. Energy Environ Sci 8:776–789
11. Genovese M, Lian K (2015) Polyoxometalate modified inorganic–organic nanocomposite materials for energy storage applications: a review. Curr Opin Solid St M 19:126–137
12. Cuentas-Gallegos AK, Gonzales-Toledo M, Rincón ME (2007) Nanocomposite hybrid material based on carbon nanofibers and polyoxometalates. Rev Mex Fis S 53:91–95
13. Cuentas-Gallegos AK, Martínez-Rosales R, Baibarac M, Gómez-Romero P, Rincón ME (2007) Electrochemical supercapacitors based on novel hybrid materials made of carbon nanotubes and polyoxometalates. Electrochem Commun 9:2088–2092
14. Baeza-Rostro DA, Cuentas-Gallegos AK (2013) Capacitance improvement of carbon aerogels by the immobilization of polyoxometalates nanoparticles. Curr Opin Solid St M 13: 203–207
15. Ruiz V, Suarez-Guevara J, Gómez-Romero P (2012) Hybrid electrodes based on polyoxometaltes-carbon materials for electrochemical supercapacitors. Electrochem Commun 24:35–38
16. Suarez-Guevara J, Ruiz V, Gómez-Romero P (2014) Hybrid energy storage: high voltage aqueous supercapacitors based on activated carbon-phosphotungstate hybrid materials. J Mater Chem A 2: 1014–1021
17. Mizuno N, Misono M (1998) Heterogeneous catalysis. Chem Rev 98:199–217
18. López-Salinas E, Hernández-Cortez JG, Shifter I, Torres-García E, Navarrete J, Gutierrez-Carrillo A, López T, Lottic PP, Bersani D (2000) Thermal stability of 12-tungstophosphoric acid supported on zirconia. Appl Catal A 193:215–225
19. Kozhevnikov IV, Sinnema A, Jansen RJJ, Pamin K, Van Bekkum H (1995) New acid catalyst comprising heteropoly acid on a mesoporous molecular sieve MCM-41. Catal Lett 30:241–252
20. Pizzio LR, Cacares CV, Blanco MN (1998) Acid catalysts prepared by impregnation of tungstophosphoric acid solutions on different supports. Appl Catal A 167:283–294
21. Edwards JC, Thiel CY, Benac B, Knifton JF (1998) Solid-state NMR and FT-IR investigation of 12-tungstophosphoric acid on TiO2. Catal Lett 51:77–83
22. Keita B, Nadjo L (1987) Electrocatalysis by electrodeposited heteropolyanions and isopolyanions. J Electroanal Chem 227: 265–270

23. Keita B, Nadjo L (1988) Surface modifications with heteropoly and isopoly oxometalates: part III. Electrode modification procedures, the necessity of proton interference during the electrodeposition of the h.e.r. catalyst. J Electroanal Chem 247:157–172
24. Cuentas-Gallegos AK, Lira-Cantú M, Casañ-Pastor N, Gómez-Romero P (2005) Nanocomposite hybrid molecular materials for application in solid state electrochemical supercapacitors. Adv Funct Mater 15:1125–1133
25. Gómez-Romero P, Chojak M, Cuentas-Gallegos K, Asensio JA, Kulesza PJ, Casañ-Pastor N, Lira-Cantú M (2003) Hybrid organic–inorganic nanocomposite materials for application in solid state electrochemical supercapacitors. Electrochem Commun 5:149–153
26. Vaillant J, Lira-Cantú M, Cuentas-Gallegos K, Casañ-Pastor N, Gómez-Romero P (2006) Chemical synthesis of hybrid materials based on PAni and PEDOT with polyoxometalates for electrochemical supercapacitors. Prog Solid State Chem 34:147–159
27. Alcañiz-Monge J, Trautwein G, Parres-Esclapez S, Maciá-Agulló JA (2008) Influence of microporosity of activated carbons as support of polyoxometalates. Microporous Mesoporous Mater 115: 440–446
28. Song Y, Wang E, Kang Z, Lan Y, Tian C (2007) Synthesis of polyoxometalates-functionalized carbon nanotubes composites and relevant electrochemical properties study. Mater Res Bull 42: 1485–1491
29. Fei B, Lu H, Hu Z, Xin JH (2006) Solubilization, purification and functionalization of carbon nanotubes using polyoxometalate. Nanotechnology 17:1589–1593
30. Kang Z, Wang Y, Wang E, Lian S, Gao L, You W, Hu C, Xu L (2004) Polyoxometalates nanoparticles:synthesis, characterization and carbon nanotube modification. Solid State Commun 129: 559–564
31. Cuentas-Gallegos AK, Jiménez-Peñaloza S, Baeza-Rostro DA, Germán-García A (2010) Influence of the functionalization degree of multiwalled carbon nanotubes on the immobilization of polyoxometalates and its effect on their electrochemical behavior. J New Mater Electrochem Syst 13:369–376
32. Cuentas-Gallegos AK, Martínez-Rosales R, Rincón ME, Hirata GA, Orozco G (2006) Design of hybrid materials based on carbon nanotubes and polyoxometalates. Opt Mater 29:126–133
33. Cuentas-Gallegos AK, Zamudio-Flores A, Casas-Cabanas M (2011) Dispersion of SiW12 nanopaticles on highly oxidized multiwalled carbon nanotubes. J Nano Res 14:11–18
34. Wang S, Li H, Li S, Liu F, Wu D, Feng X, Wu L (2013) Electrochemical-reduction-assisted assembly of a polyoxometalate/graphene nanocomposite and its enhanced lithium-storage performance. Chem Eur J 19:10895–10902
35. Tessonnier JP, Goubert-Renaudin S, Alia S, Yan Y, Barteau MA (2012) Structure, stability, and electronic interactions of polyoxometalates on functionalized graphene sheets. Langmuir 29:393–402
36. Fernandes DM, Freire C (2014) Carbon nanomaterial-phosphomolybdate composites for oxidative electrocatalysis. ChemElectroChem 2:269–279
37. Petit C, Bandosz TJ (2009) Graphite oxide/polyoxometalate nanocomposite as adsorbents of ammonia. J Phys Chem C 113:3800–3809
38. Cheng L, Liu J, Dong S (2000) Layer-by-layer assembly of multilayer films consisting of silicotungstate and a cationic redox polymer on 4-aminobenzoic acid modified glassy carbon electrode and their electrocatalytic effects. Anal Chim Acta 417:133–142
39. Martel D, Gross M (2007) Electrochemical study of multilayer films built on glassy carbon electrode with polyoxometalate anions and two multi-charged molecular cationic species. J Solid State Electr 11:421–429
40. Garrigue P, Delville MH, Labrugere C, Cloutet E, Kulesza PJ, Morand JP, Kuhn A (2004) Top-down approach for the preparation of colloidal carbon nanoparticles. Chem Mater 16:2984–2986
41. Stein A, Wang A, Flarke MA (2009) Functionalization of porous carbon materials with designed pore architecture. Adv Mater 21: 265–293
42. Pech D, Guay D, Brousse T, Bélanger D (2008) Concept for charge storage in electrochemical capacitors with functionalized carbon electrodes. Electrochem Solid St 11:A202–A205
43. Toupin M, Bélanger D (2008) Spontaneous functionalization of carbon black by reaction with 4-nitrophenyldiazonium cations. Langmuir 24:1910–1917
44. Pognon G, Brousse T, Demarconnay L, Bélanger D (2011) Performance and stability of electrochemical capacitor based on anthraquinone modified activated carbon. J Power Sources 196: 4117–4122
45. Lu M, Nolte WM, He T, Corley DA, Tour JM (2009) Direct covalent grafting of polyoxometalates onto Si surfaces. Chem Mater 21: 442–446
46. Gamelas JAF, Evtuguin DV, Esculcas AP (2007) Transition metal substituted polyoxometalates supported on amine-functionalized silica. Transit Met Chem 32:1061–1067
47. Zhang X, Wu W, Wang J, Liu C, Quian S (2008) Molybdenum polyoxometalate impregnated amino-functionalized mesoporous silica thin films as multifunctional materials for photochromic and electrochemical applications. J Mater Res 23:18–26
48. Balamurugan A, Chen SM (2007) Silicomolybdate doped polypyrrole film modified glassy carbon electrode for electrocatalytic reduction of Cr(VI). J Solid State Electr 11:1679–1687
49. Fernandes DM, Brett CMA, Cavaleiro AMV (2011) Layer-by-layer self-assembly and electrocatalytic properties of poly(ethylenimine)-silicotungstate multilayer composite films. J Solid State Electr 15: 811–819
50. Lyskawa J, Gronde A, Belanger D (2010) Chemical modifications of carbon powders with aminophenyl and cyanophenyl groups and a study of their reactivity. Carbon 48:1271–1278
51. Obradovic MD, Vukovic GD, Stevanovic SI, Panic VV, Uskokovic PS, Kowal A, SLJ G (2009) A comparative study of the electrochemical properties of carbon nanotubes and carbon black. J Electroanal Chem 634:22–30
52. Hernández López S, Santiago Enrique V (2013) In: Hany A El-Shemy, InTech (ed) Soybean Oil-Based Polymers, ISBN 978–953–51–0977–8
53. Mayo DW, Miller FA, Hannah RW (2004) Course notes on the interpretation of infrared and Raman spectra. John Wiley & Sons, Inc,, Hoboken
54. Larkin P (2011) Infrared and Raman spectroscopy: principles and spectral interpretation. Elsevier, USA
55. Kumar NA, Choi HJ, Shin YR, Chang DW, Dai L, Baek JB (2012) Polyaniline-grafted reduced graphene oxide for efficient electrochemical supercapacitors. ACS Nano 6:1715–1723
56. Li Y, Wang J, Li X, Geng D, Li R, Sun X (2011) Superior energy capacity of graphene nanosheets for a nonaqueous lithium-oxygen battery. Chem Commun 47:9438–9440
57. Buffa F, Hu H, Resasco DE (2005) Side-wall functionalization of single-walled carbon nanotubes with 4-hydroxymethylaniline followed by polymerization of ∈ − caprolactone. Macromolecules 38:8258–8263
58. Raymundo-Piñero E, Leroux F, Béguin F (2006) A high-performance carbon for supercapacitors obtained by carbonization of a seaweed biopolymer. Adv Mater 18:1877–1882
59. Frackowiak E, Béguin F (2001) Carbon materials for the electrochemical storage of energy in capacitors. Carbon 39:937–950
60. Li H, Xi H, Zhu S, Wen Z, Wang R (2006) Preparation, structural characterization, and electrochemical properties of chemically

modified mesoporous carbon. Microporous Mesoporous Mater 96:357–362
61. Zhou Z, Zhang Z, Peng H, Qin Y, Li G, Chen K (2014) Nitrogen- and oxygen-containing activated carbon nanotubes with improved capacitive properties. RCS Adv 4:5524–5530
62. Santos LM, Ghilane J, Fave C, Lacaze PC, Randriamahazaka H, Abrantes LM, Lacroix JC (2008) Electrografting polyaniline on carbon through the electroreduction of diazonium salts and the electrochemical polymerization of aniline. J Phys Chem C 112:16103–16109
63. Sharma LR, Manchanda AK, Singh G, Verma RS (1982) Cyclic voltammetry of aromatic amines in aqueous and Non-aqueous media. Electrochim Acta 27:223–233
64. Bélanger D, Pinson J (2011) Electrografting: a powerful method for surface modification. Chem Soc Rev 40:3995–4048
65. Isikli S, Díaz R (2012) Substrate-dependence performance of supercapacitors based on an organic redox couple impregnated carbon. J Power Sources 206:53–58
66. Martel D, SOjic N, Kuhn A (2002) A simple student experiment for teaching surface electrochemistry: adsorption of polyoxometalate on graphite electrodes. J Chem Educ 79:349–352
67. Timofeeva MN (2003) Acid catalysis by heteropoly acids. Appl Catal A 256:19–35
68. Vairalakshmi M, Raj V, Sami P, Rajasekaran K (2011) Studies on electron transfer reactions: oxidation of phenol and ring-substituted phenols by heteropoly 11-tungstophosphovanadate(V) in aqueous acidic medium. Transit Met Chem 36:875–882
69. Manivel A, Asiri K, Alamry KA, Lana-Villarreal T, Anandan S (2014) Interfacially synthesized PAni-PMo12 hybrid material for supercapacitor applications. B Mater Sci 37:861–869
70. Papagianni GG, Stergiou DV, Armatas GS, Kanatzidis MG, Prodromidis MI (2012) Synthesis, characterization and performance of polyaniline–polyoxometalates (XM12, X=P;Si and M=Mo,W) composites as electrocatalysts of bromates. Sensor Actuat B-Chem 173:346–353